

Attention W-Net: Improved Skip Connections for Better Representations

Shikhar Mohan*, Saumik Bhattacharya* and Sayantari Ghosh†

* Indian Institute of Technology Kharagpur, India

† National Institute of Technology Durgapur, India

Abstract—Segmentation of macro and microvascular structures in fundoscopic retinal images plays a crucial role in the detection of multiple retinal and systemic diseases, yet it is a difficult problem to solve. Most neural network approaches face several issues such as lack of enough parameters, overfitting and/or incompatibility between internal feature-spaces. We propose Attention W-Net, a new U-Net based architecture for retinal vessel segmentation to address these problems. In this architecture, we have two main contributions: Attention Block and regularisation measures. Our Attention Block uses attention between encoder and decoder features, resulting in higher compatibility upon addition. Our regularisation measures include augmentation and modifications to the ResNet Block used, which greatly prevent overfitting. We observe an F1 and AUC of 0.8407 and 0.9833 on the DRIVE and 0.8174 and 0.9865 respectively on the CHASE-DB1 datasets — a sizeable improvement over its backbone as well as competitive performance among contemporary state-of-the-art methods.

I. INTRODUCTION

Learned medical image segmentation is a research area that has been receiving a great deal of attention in the computer vision community. Traditionally, medical experts have been analysing these various forms of medical images ranging from X-Ray, Ultrasound Imaging, Computed Tomography (CT), Magnetic Resonance Imaging (MRI), Fundoscopic Imaging, etc. to manually generate dense labels. The above being a tedious, error-prone and expensive task, a computer-aided diagnosis is a natural solution. Deep learning based methods, more specifically CNN based architectures, have come very far in solving these problems. Many architectures such as FCN [1] and U-Net [2] have given rise to models that have grown in popularity for such tasks due to their near-radiologist performances and much higher efficiency. In this paper, we focus on the Retinal Blood Vessel Segmentation task using fundoscopic images. These images serve as an essential *in vivo* test for detecting retinal diseases as well as systemic diseases (such as high blood pressure, diabetic retinopathy, and microvascular complications of diabetes). Therefore, accurate segmentation of retina blood vessels is an essential task.

The most significant difficulty in the vessel segmentation task is the insignificant difference between the pixels belonging to the vessels and the pixels belonging to the background, followed by the thinness of microvessels at the ends and edges. The true scope of this difficulty can be realised when we consider the noise present in these images and optic disks (bright spots) present in retinal fundus images. Much of this noise can be attributed to poor illumination, sensor noise

and incorrect filters and angles used in fundus cameras. The limited amount of retinal data is a sizeable hurdle as well. In fact, there are less than 25 images available for training in publicly available datasets, *i.e.* CHASE-DB1 [3], DRIVE [4] and STARE [5].

Deep learning has revolutionized various areas in computer vision and biomedical image understanding is no exception. Neural networks have brought about state-of-the-art performance in multiple challenges, and CNN based architectures have done the same in computer vision. Among CNN based neural networks, U-Net [2] based architectures have been receiving a lot of attention for biomedical image segmentation tasks due to these networks consisting of an encoder to decoder structure with skip connections which allow for an efficient flow of gradients for learning. The encoder captures context information whereas the decoder enables precise localisation based on the task.

Many other research works investigate different aspects of this task, such as *Uysal et. al.* [6] highlights the importance of image augmentation in this task. [6] investigates not only affine transforms but also transforms in the pixel subspace as well as elastic transforms. SGL [7] aims to improve the robustness of the model since it is effectively trained on noisy labels due to clinicians' manual labelling. GANs have been employed for this task as well, where RV-GAN [8] introduces a feature matching loss to ameliorate the type-1 error caused by thresholding segmentation heatmaps to generate segmentation maps. Attention based techniques, which find their origin in language processing (NLP) for image captioning [9], machine translation and comprehension tasks [10], have garnered interest for this task as well. SA-UNet [11] introduces a spatial attention module at the bottom-most layer for adaptive feature refinement. This attention module aims at suppressing unimportant features and enhancing more important features. Attention U-Net [12] introduces a modified grid-based attention module at every layer. This form of attention gating filters gradients in the forward as well as the backward pass.

However, most of the above approaches struggle with some common issues. Most of the above networks do not have enough parameters to learn the necessary complex features. This can be observed in that these networks primarily struggle to segment microvessels at the end of larger vessels in the fundus images. In networks which do have more parameters such as LadderNet [13] we observe sizeable overfitting, but

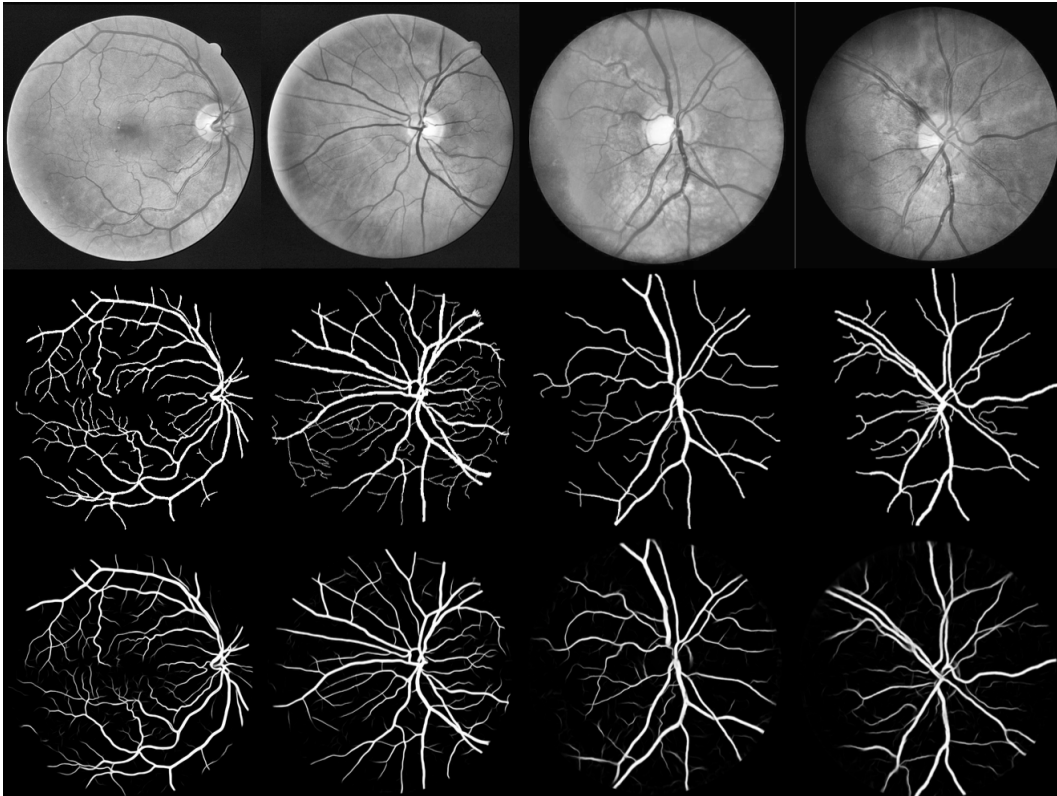


Fig. 1. First two columns are from DRIVE and the second two are from CHASE-DB1. For rows from top to bottom, the labels are (a) Original Image (b) Ground Truth (c) Attention W-Net (ours) Prediction

the detachment from the basic encoder-decoder architecture is a step in the right direction. Even though skip-connections are the reason why U-Net architectures work so well, the difference in feature-spaces between the encoder features and decoder features results in sub-optimal representation learning in all of the aforementioned architectures. Taking all of the above into account, we introduce Attention W-Net. The two key motivators of our work are to help the signal from the encoder branch stay relevant in the decoder branch and to add a meaningful regularisation signal to our training process as well. Hence, the main contributions of our work are as follows:

- An Attention Block that magnifies the utility of skip connections and ensures learning of richer features by preserving the relevance of the encoder features in the decoding branch.
- A meaningful regularising signal in the form of careful image augmentations and the construction of a Residual Block to prevent our network from overfitting.
- A Retina Blood Vessel segmentation model with top performance.

II. PROPOSED METHODOLOGY

The Attention W-Net employs LadderNet as a backbone network, on top of which we add our modified Attention Blocks. The LadderNet framework we employ has two alter-

nating encoder branches and decoder branches, which make the structure akin to two U-Nets. The Residual Block is present at every level, whereas the Attention Block is present only in the two upsampling phases of the network, ensuring smooth integration of the encoder signal from the skip-connections into the decoder layers. In the end, we use Binary Cross-Entropy loss to compute the loss. For pixel i with prediction \hat{y}_i and ground truth y_i , we have L_i as the value of the cost function as follows:

$$L_i = -y_i \log(\hat{y}_i) - (1 - y_i) \log(1 - \hat{y}_i) \quad (1)$$

A. Attention Block

In most U-Net based architectures the encoder branch focuses on extracting high-dimensional features from the data, whereas the decoder branch focuses on rearranging and localising these features to achieve the goal at hand – image segmentation in this case. It has been very well observed that the decoding process benefits from being able to incorporate the encoder signal as well, which is implemented by summing or concatenating the encoder features using skip-connections. However, it is easy to see that these features, if used directly, would be incompatible to some extent due to the innate differences between the two feature spaces at hand.

To tackle this issue, we introduce our Attention Block. The structure is similar to the counterpart found in [12],

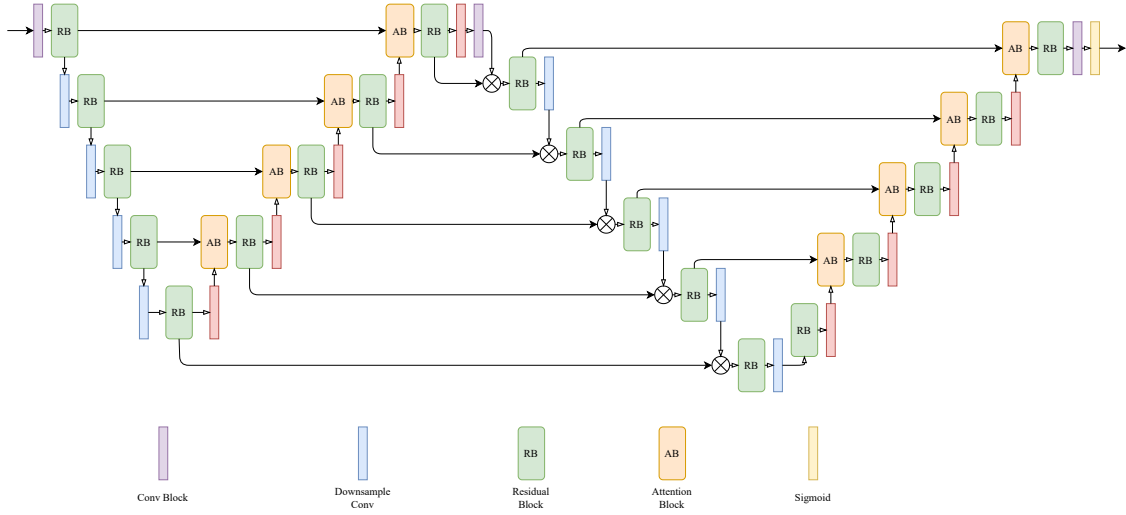


Fig. 2. Attention W-Net Network Structure

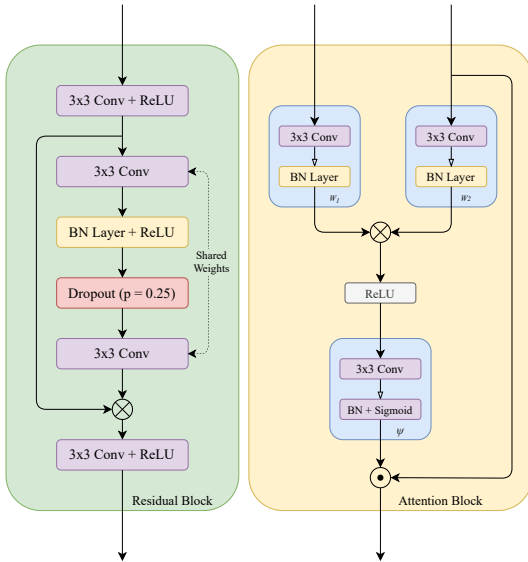


Fig. 3. Residual Block (left) and Attention Block (right).

except we attend over the encoder features using the decoder features, and add the resultant features for further decoding. The difference between the two is substantial as the former results in the encoder signal being drowned out as it is only used to attend over the decoder signal. Formally, we state that $g^{k-1} \in \mathbb{R}^{H \times W \times C_k}$ and $x^{k-1} \in \mathbb{R}^{H \times W \times C_k}$ are the encoder and decoder feature outputs respectively from the $(k-1)^{\text{th}}$ layer, W_1 , W_2 and ϕ are convolutional blocks in the Attention Block. Now we have,

$$p^{k-1} = \psi(\text{ReLU}(W_1(g^{k-1}) + W_2(x^{k-1}))) \quad (2)$$

Here, p^{k-1} denotes the attention map generated from encoder and decoder features from the $(k-1)^{\text{th}}$ layer. All values in

p^{k-1} are in $(0, 1)$. This attention map is then applied to the encoder feature as follows:

$$g_d^{k-1} = g^{k-1} \odot p^{k-1} \quad (3)$$

Where g_d^{k-1} is the attended encoder feature and \odot denotes element-wise multiplication. Now that g_d^{k-1} contains information regarding the decoder feature in it as well, we have $x_d^{k-1} = g_d^{k-1} + x^{k-1}$ where x_d^{k-1} represents the summed up feature which is then sent to the k^{th} layer in the decoder network.

B. Regularisation

Most U-Net based architectures for this task are prone to overfitting, and to solve this problem we emphasize the importance of not only standard regularising methods but meaningful ones as well. In this section, we discuss two components of our work: the Residual Block and our careful image augmentation. The importance of meaningful regularisation is emphasized in this task more than others due to the sheer unavailability of data as well as the defects found therein.

The Residual Block we use is inspired by the ResNet [14] Basicblock, with minor modifications. Majorly, it uses only two convolutional layers, which share weights (as in LadderNet), except with added BatchNorm layers to the official LadderNet implementation. The shared weights between the two convolutional layers make for easier learning of features, in between which we add a dropout layer to prevent overfitting. This Residual Block has a lesser number of parameters than a standard ResNet Basicblock, and the residual connection, dropout layer and the BatchNorm layers result in an effective regularisation, which helps us take advantage of the large number of parameters we include in this network to learn richer representations without overfitting.

Note that this doesn't contradict with the idea that our intention here is to make a deeper network. This is because in many

TABLE I
RANDOM DATA AUGMENTATIONS USED WITH PROBABILITIES

Data Augmentations Used	Probability
Random Sized Crop with Padding	0.5
Vertical Flip	0.5
Rotate 90°	0.5
Elastic Transform	0.5
Grid Distortion	0.5
Optical Distortion	0.8
Brightness Contrast	0.8
Random Gamma	0.8

cases, the shallower networks do not have enough capacity to directly perform the segmentation task, and they are often combined with a deeper module or a refinement module [15], [16]. Thus, it is important to design the network with sufficient depth. This being said, removing the weight sharing in the residual blocks significantly degrades our performance (8-12% performance drop in terms of F1-score on DRIVE dataset). Thus, the proposed model is designed after performing careful ablation studies keeping a trade-off between the number of parameters and the performance of the model.

In addition to this, we use careful image augmentation as well in our training process. Table I details the image augmentation techniques we use. These carefully selected image augmentations make our network robust to the naturally occurring distortions in the dataset as well as increase its statistical size.

III. EXPERIMENTS

In this section, we provide a detailed description of the experimental design, the results and the comparisons. The experiments have been performed on a Windows workstation, which has a single NVIDIA GeForce RTX 2080 with 8GB VRAM and Intel Core i5-9600K CPU. We use a PyTorch as our framework of choice to design and train our architectures.

A. Data

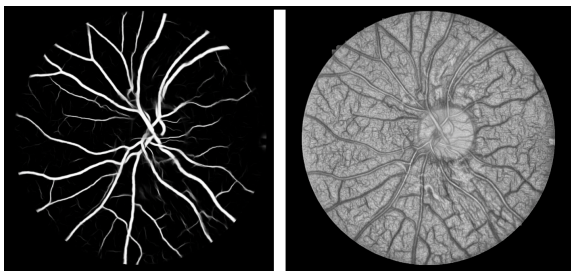


Fig. 4. Prediction (left) vs. Seg-Grad-Cam visualisation (right).

In the Retina Vessel Segmentation, the most widely used datasets are the DRIVE [4] and CHASE-DB1 [3] datasets. The DRIVE dataset contains 20 training and 20 testing images in *.tif* (565×584), whereas the CHASE-DB1 dataset had 20 training and 8 testing images in *.jpg* (999×960) format. For

both the datasets, we extract patches of size 48×48 and use 10% of training samples as validation data. For both inference and training, overlapping patches are extracted, after which we apply the FOV (field of view) masks. The official FOVs are not provided in the case of the CHASE-DB1 dataset, so we extract them from the original images with methods same as in IterNet [17].

B. Training Setup

We choose a LadderNet backbone with 5 levels, resulting in 1419636 parameters and the value of dropout was set to 0.25. We evaluate the segmentation loss using binary cross-entropy loss and applied the Adam optimizer with default parameters and a batch size of 1024. We used a “reduce learning rate on plateau” strategy for learning rate scheduling, where we train with the rate 10^{-3} for 100 epochs and 10^{-4} for the rest of the training process, which goes on for 250 epochs in total. For the CHASE-DB1 dataset, we train for 50 more epochs with a learning rate 5×10^{-5} to compensate for the larger image size leading to a larger training set.

We tried different loss terms, like l_1 and l_2 losses, for the segmentation task. However, BCE loss has performed significantly better than the other loss terms. This is in line with the recent SOTA methods [13], [18], [19] where BCE loss and its variants have performed significantly better than the conventional l_p norm based losses in segmentation tasks.

We use carefully chosen randomized data augmentation for this training process as well. The data augmentations we used along with probability values can be seen in Table I. The entire training process takes nearly 15 hours.

C. Inference

During inference, we use a patch-width of 48 and stride length 5 to obtain our results. This setting implies 89.6% overlap between the patches. For a pixel, all the predicted values are averaged over all patches that include the given pixel to determine the true prediction. This brings better predictions in our experiments, at the cost of computational overhead. We observe that averaging produces an ensembling-like effect and maintains continuity for the thin microvessels present, which is primarily why higher overlap corresponds to better performance.

D. Quantitative Bench-marking

We compare our architecture with multiple formative as well as state-of-the-art architectures on the bases of F1-score, AUC-ROC and Accuracy. We perform this comparison over the DRIVE and CHASE-DB1 datasets using their publicly available codebases. Our method might not achieve state-of-the-art performance on these metrics but it is important to note that we base our Attention-Block architecture on top of the LadderNet network, which means the magnitude of improvement in metrics over LadderNet is what we give more importance to. Figure 4 shows raw predictions and (monochrome) attention heatmap for a sample image from the

TABLE II
COMPARISON ON THE DRIVE AND CHASE-DB1 DATASETS.

Method	F1-Score	ACC	AUC
DRIVE			
DU-Net [21]	0.8174	0.9555	0.9752
Recurrent UNet [22]	0.8155	0.9556	0.9782
Residual UNet [22]	0.8149	0.9553	0.9779
R2U-Net [23]	0.7928	0.9556	0.9634
LadderNet [13]	0.8202	0.9561	0.9793
IterNet [17]	0.8205	0.9573	0.9816
AG-Net [24]	-	0.9692	0.9864
SA-UNet [11]	0.8263	0.9698	0.9864
SGL [7]	0.8316	-	0.9886
<i>Uysal et. al.</i> [6]	-	0.9712	0.9855
AW-Net (Ours)	0.8407	0.9588	0.9833
CHASE-DB1			
DU-Net [21]	0.7853	0.9724	0.9863
Residual U-Net [22]	0.7800	0.9553	0.9779
Recurrent U-Net [22]	0.7810	0.9622	0.9803
R2U-Net [23]	0.7928	0.9634	0.9815
LadderNet [13]	0.8031	0.9656	0.9839
IterNet [17]	0.8073	0.9655	0.9851
SA-UNet [11]	0.8151	0.9755	0.9905
AW-Net (ours)	0.8174	0.9689	0.9865

CHASE-DB1 dataset. The heatmap is generated using Seg-Grad-Cam [20].

We see that our model has notable gains over the initial LadderNet architecture in all three metrics, which tells us that our novel additions sizeably improve learning. Accuracy being one of the least reliable metrics for image segmentation, we believe it is logical to give more importance to F1-Score and AUC metrics. For most models from IterNet [17] onwards (including ours), we note very good performance in terms of AUC (≥ 0.97), but we see that there is very little variance. However, there is a significantly higher disparity in F1-Scores, which is where our model excels. It is to be noted that our proposed model outperforms even the most recent approaches. Thus, these benchmarks prove that our novel additions help our backbone capture richer representations, leading to better segmentation performance.

E. Improvement Analysis

In this section, we demonstrate the significance of improvement over the LadderNet backbone. We do this in two ways, first by conducting a statistical significance test over 5 identical runs with only differing randomisation seeds and second by comparing ROC curves, Figure 5.

With 4 degrees of freedom, we conduct a *paired t-Test* with a one-tailed distribution, through which for both F1-Score and AUC, we reject the null hypothesis (with $\alpha = 0.005$). We find p-values for the former to be 5.55×10^{-6} and for the latter to be 3.81×10^{-4} , which confirm that our

TABLE III
TESTS FOR STATISTICAL SIGNIFICANCE

LadderNet		Ours	
F1-Score	AUC	F1-Score	AUC
0.8202	0.9793	0.8407	0.9833
0.8195	0.9801	0.8390	0.9835
0.8210	0.9812	0.8374	0.9844
0.8203	0.9785	0.8397	0.9844
0.8191	0.9790	0.8389	0.9824

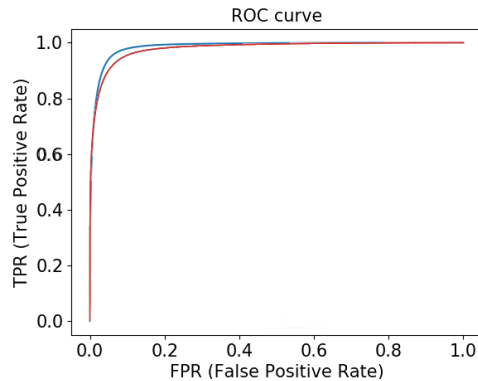


Fig. 5. ROC curves for LadderNet (red) and Attention W-Net (blue).

improvements over LadderNet are statistically significant for both the aforementioned metrics.

F. Ablation Study

In this section, we perform an ablation study, where we make use of the DRIVE dataset and make small changes to the network, keeping the rest of the training procedure invariant. The training procedure we adopt is the same as in Sec. III-B, i.e. for 250 epochs with “reduce LR on plateau” learning rate scheme, starting with 0.01. Note that without any of our novel elements, we essentially have the LadderNet architecture, which is the starting point of our ablation study.

We demonstrate the impact of our three contributions: ResBlock modification, Regularisation and Attention Block (AB). To understand the effects of our proposed blocks, we add them sequentially to the backbone model to investigate the improvements achieved in each step. Additionally, we also show how our design of the Attention Block – which we refer to as Type-2 – is superior in performance to the traditional design (as in AG-Net [24]) which we refer to as Type-1. Maintaining the same definitions from Sec. II-A, Type-1 AB can be formally characterized by computing x_d^k (the k^{th} layer decoder input) differently from Type-2 AB. Instead of (3), we have $x_d^k = p^{k-1} \odot x^{k-1}$. The calculated x_d^k is then directly sent to the k^{th} decoder layer. We can see that with each subsequent (orthogonal) addition of a component, there is a noticeable performance improvement. This proves that each of our components contributes sizeably to the final performance.

TABLE IV
ABLATION OF DIFFERENT MODELS.

ResBlock	Augmentation	AB	F1	AUC
✗	✗	✗	0.8202	0.9793
✓	✗	✗	0.8250	0.9806
✓	✓	✗	0.8275	0.9828
✓	✓	Type-1	0.8322	0.9809
✓	✓	Type-2	0.8407	0.9833

IV. CONCLUSIONS

In this paper we present a novel architecture Attention W-Net, which is focuses on improving gradient flow in U-Net based architectures. We achieve the same in two ways, firstly by improving skip connections by attending over the encoder signal using the decoder features so that them being summed up results in a more meaningful signal as the decoder branch restructures the high dimensional features expanded by the encoder branch into segmentation maps. Secondly, we incorporate a modified Residual Block and use careful image augmentation to add a meaningful regularisation signal to our training process. The Residual Block helps in preventing overfitting by using Shared Weights, dropout and BatchNorm layers, whereas the image augmentation ameliorates the issues arising from having less data by making the model more robust to distortions by injecting the same stochastically into the training process. Our model has a sizeable performance gain over the backbone LadderNet, proving the utility of our novelty, and showcases top performance among the latest architectures as well.

REFERENCES

- [1] J. Long, E. Shelhamer, and T. Darrell, "Fully convolutional networks for semantic segmentation," in *Proceedings of the IEEE conference on computer vision and pattern recognition*, 2015, pp. 3431–3440. 1
- [2] O. Ronneberger, P. Fischer, and T. Brox, "U-net: Convolutional networks for biomedical image segmentation," in *International Conference on Medical image computing and computer-assisted intervention*. Springer, 2015, pp. 234–241. 1
- [3] M. M. Fraz, P. Remagnino, A. Hoppe, B. Uyyanonvara, A. R. Rudnicka, C. G. Owen, and S. A. Barman, "An ensemble classification-based approach applied to retinal blood vessel segmentation," *IEEE Transactions on Biomedical Engineering*, vol. 59, no. 9, pp. 2538–2548, Sep. 2012. 1, 4
- [4] J. Staal, M. Abramoff, M. Niemeijer, M. Viergever, and B. van Ginneken, "Ridge based vessel segmentation in color images of the retina," *IEEE Transactions on Medical Imaging*, vol. 23, no. 4, pp. 501–509, 2004. 1, 4
- [5] A. D. Hoover, V. Kouznetsova, and M. Goldbaum, "Locating blood vessels in retinal images by piecewise threshold probing of a matched filter response," *IEEE Transactions on Medical Imaging*, vol. 19, no. 3, pp. 203–210, March 2000. 1
- [6] E. S. Uysal, M. Ş. Bilici, B. S. Zaza, M. Y. Özgenc, and O. Boyar, "Exploring the limits of data augmentation for retinal vessel segmentation," *arXiv preprint arXiv:2105.09365*, 2021. 1, 5
- [7] Y. Zhou, H. Yu, and H. Shi, "Study group learning: Improving retinal vessel segmentation trained with noisy labels," *arXiv preprint arXiv:2103.03451*, 2021. 1, 5
- [8] S. A. Kamran, K. F. Hossain, A. Tavakkoli, S. L. Zuckerbrod, K. M. Sanders, and S. A. Baker, "Rv-gan: retinal vessel segmentation from fundus images using multi-scale generative adversarial networks," *arXiv preprint arXiv:2101.00535*, 2021. 1
- [9] P. Anderson, X. He, C. Buehler, D. Teney, M. Johnson, S. Gould, and L. Zhang, "Bottom-up and top-down attention for image captioning and visual question answering," in *Proceedings of the IEEE Conference on Computer Vision and Pattern Recognition (CVPR)*, June 2018. 1
- [10] T. Shen, T. Zhou, G. Long, J. Jiang, S. Pan, and C. Zhang, "Disan: Directional self-attention network for rnn/cnn-free language understanding," in *Proceedings of the AAAI conference on artificial intelligence*, vol. 32, 2018. 1
- [11] C. Guo, M. Szemenyei, Y. Yi, W. Wang, B. Chen, and C. Fan, "SUNET: Spatial attention u-net for retinal vessel segmentation," in *2020 25th International Conference on Pattern Recognition (ICPR)*. IEEE, 2021, pp. 1236–1242. 1, 5
- [12] O. Oktay, J. Schlemper, L. L. Folgoc, M. Lee, M. Heinrich, K. Misawa, K. Mori, S. McDonagh, N. Y. Hammerla, B. Kainz *et al.*, "Attention u-net: Learning where to look for the pancreas," *arXiv preprint arXiv:1804.03999*, 2018. 1, 2
- [13] J. Zhuang, "Laddernet: Multi-path networks based on u-net for medical image segmentation," *arXiv preprint arXiv:1810.07810*, 2018. 1, 4, 5
- [14] K. He, X. Zhang, S. Ren, and J. Sun, "Deep residual learning for image recognition," in *Proceedings of the IEEE conference on computer vision and pattern recognition*, 2016, pp. 770–778. 3
- [15] L. Zhang, G. Yang, and X. Ye, "Automatic skin lesion segmentation by coupling deep fully convolutional networks and shallow network with textons," *Journal of Medical Imaging*, vol. 6, no. 2, p. 024001, 2019. 4
- [16] H. Zhang, K. Dana, J. Shi, Z. Zhang, X. Wang, A. Tyagi, and A. Agrawal, "Context encoding for semantic segmentation," in *Proceedings of the IEEE conference on Computer Vision and Pattern Recognition*, 2018, pp. 7151–7160. 4
- [17] L. Li, M. Verma, Y. Nakashima, H. Nagahara, and R. Kawasaki, "Iternet: Retinal image segmentation utilizing structural redundancy in vessel networks," in *Proceedings of the IEEE/CVF Winter Conference on Applications of Computer Vision*, 2020, pp. 3656–3665. 4, 5
- [18] L. Li, X. Weng, J. A. Schnabel, and X. Zhuang, "Joint left atrial segmentation and scar quantification based on a dnn with spatial encoding and shape attention," in *International Conference on Medical Image Computing and Computer-Assisted Intervention*. Springer, 2020, pp. 118–127. 4
- [19] J. Su, Z. Liu, J. Zhang, V. S. Sheng, Y. Song, Y. Zhu, and Y. Liu, "Dv-net: Accurate liver vessel segmentation via dense connection model with d-bce loss function," *Knowledge-Based Systems*, vol. 232, p. 107471, 2021. 4
- [20] K. Vinogradova, A. Dibrov, and E. W. Myers, "Towards interpretable semantic segmentation via gradient-weighted class activation mapping," in *Proceedings of the AAAI Conference on Artificial Intelligence*, 2020. 5
- [21] Q. Jin, Z. Meng, T. D. Pham, Q. Chen, L. Wei, and R. Su, "Dunet: A deformable network for retinal vessel segmentation," *Knowledge-Based Systems*, vol. 178, pp. 149–162, 2019. 5
- [22] L.-C. Chen, G. Papandreou, I. Kokkinos, K. Murphy, and A. L. Yuille, "Deeplab: Semantic image segmentation with deep convolutional nets, atrous convolution, and fully connected crfs," *IEEE transactions on pattern analysis and machine intelligence*, vol. 40, no. 4, pp. 834–848, 2017. 5
- [23] M. Z. Alom, M. Hasan, C. Yakopcic, T. M. Taha, and V. K. Asari, "Recurrent residual convolutional neural network based on u-net (r2u-net) for medical image segmentation," 2018. 5
- [24] S. Zhang, H. Fu, Y. Yan, Y. Zhang, Q. Wu, M. Yang, M. Tan, and Y. Xu, "Attention guided network for retinal image segmentation," in *International Conference on Medical Image Computing and Computer-Assisted Intervention*. Springer, 2019, pp. 797–805. 5